# DIRECT AND RAPID DESCRIPTION OF THE INDIVIDUAL IONIC CURRENTS OF SQUID AXON MEMBRANE BY RAMP POTENTIAL CONTROL

HARVEY M. FISHMAN

*From the Laboratory of Biophysics, National Institute of Neurological Diseases and Stroke, National Institutes of Health, Bethesda, Maryland 20014 and the Marine Biological Laboratory, Woods Hole, Massachusetts 02543*

ABSTRACT Computations based upon the Hodgkin-Huxley equations and experimental data from squid axons show that ramp functions can be used as commands to a voltage clamp system to selectively observe either the fast (sodium) or slow (potassium) process in axon membranes without chemical separation techniques or computer assistance. Each process is characterized directly (on line) and rapidly (real time) by generating a current-potential curve on an oscilloscope for fast or slow rates of change of membrane potential (ramps). The speed and directness of this method of characterizing each of the essential axonal events permit quantitative measurement of the kinetics of rapid effects on these processes due to various pharmacological agents such as tetrodotoxin and tetraethylammonium ion or other experimental changes in the membrane environment.

## INTRODUCTION

The Hodgkin-Huxley (HH) formulation (1952) presently gives the most complete description of squid axon membrane behavior. This generalized (HH) axon is a convenient and useful analog from which nearly all the classical physiological properties of an axon can be computed—once the HH parameters have been determined. Unfortunately, these parameters are obtained only after tedious processing of step-voltage clamp data, or at best after an experiment by off-line computer analysis (Hille, 1967).

As step-voltage clamp procedures (Moore and Cole, 1963) have been applied to more and different membrane preparations, there has been an increasing tendency to draw conclusions from the current-potential ($I$-$V$) relations (Fig. 1) for the late steady-state ($I_{ss}$) and early transient maxima ($I_{pk}$) currents which under normal conditions give the potassium and sodium conductance characteristics. Although the negative slope in the latter curve does not represent a physical negative conductance[1] attained by the membrane, there have been enough, and important

[1] Adjacent points on this curve do not represent continuous physical states of the system, since one point cannot be reached from another by a small perturbation of an independent variable.

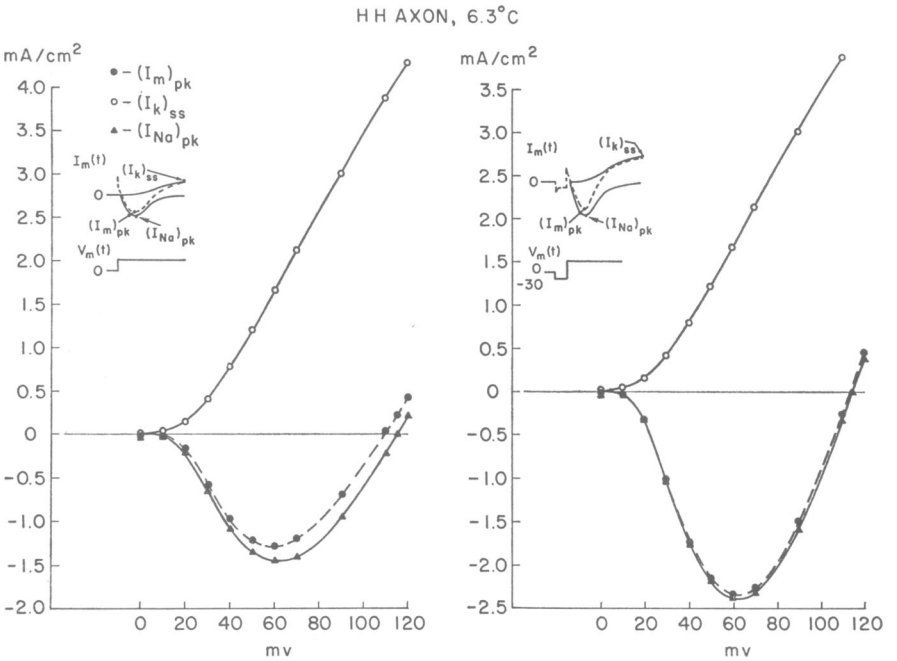


FIGURE 1 *I-V* relations for the early transient $(I_{Na})_{pk}$, late steady-state $(I_K)_{ss}$, and total peak membrane current $(I_m)_{pk}$ computed from the Hodgkin-Huxley equations for step changes from the resting potential (left) and for a hyperpolarizing 30 mv step followed 30 msec later by depolarizing steps (right). Note that the hyperpolarizing prepulse produces an increase in $(I_{Na})_{pk}$ such that a larger $g_{Na}$ is detected, and it also delays the outward $I_K$ so that $(I_m)_{pk}$ is essentially $(I_{Na})_{pk}$. The potential axis for this and subsequent figures on an HH axon is plotted as deviation from the resting potential.

enough, conclusions drawn from such an $I_{pk}$-$V$ presentation of step clamp data to thoroughly justify this procedure (cf. Cole, 1968). Consequently, it is useful to obtain these data as directly and expeditiously as possible.

Measurements and computations, which were described briefly elsewhere (Fishman and Cole, 1969; Fishman, 1969), show that such data can be obtained on line and in real time (i.e. directly and rapidly from an oscilloscope during an experiment) without computer assistance using rising or falling (ramp) voltage clamp pulses. These measurements were suggested by the fast ramp voltage clamp measurements in frog skin by Fishman and Macey (1969) and the steady-state $I(V)$ measurements on squid axon by Cole and Moore (1960).

The $I(V)$ relations in real axons and an HH axon for ramp pulses with slow and fast linear sweeps of potential give good qualitative agreement. Computations of the ionic components of current for particular ramp slopes on an HH axon show that slow ramps produce an approximate steady-state (potassium) current vs. membrane–potential relation. Similarly, fast ramps preceded by a hyperpolarizing step of 30 mv give an early transient (sodium) $I(V)$ curve. Ramp voltage clamping of

real axons confirmed these computations. Thus it is possible to selectively follow and record specific ion (either the fast or slow) processes in axons by choosing the proper ramp slope. The speed and directness of this method of characterizing the fast and slow axonal events permit quantitative measurement of the kinetics of rapid alterations in these processes following exposure to various pharmacological agents or other experimental changes in the axon membrane.

## MATERIALS AND METHODS

### *Preparation*

Woods Hole squid (*Loligo pealei*) axons (386–579 $\mu$) were used in these experiments. A 4 cm length of connective tissue in which the hindmost stellar nerve was embedded was tied off and removed from the mantle under cold running seawater. Most of the connective tissue was cleaned from the giant fiber in a separate operation with care being taken not to cut the collateral fibers emanating from the axon too short. The roughly dissected preparation could be stored for several hours in a refrigerator before the fine dissection and subsequent experiment.

### *Chamber*

The chamber was designed and has been used for several years in our laboratory but has not yet been described in detail. An axon was placed horizontally across a Lucite chamber (Rojas and Ehrenstein, 1965) with a 1.5 cm length under flowing, cold seawater. Posts on each side of the chamber supported the axon and were the entry points for the perfusion pipette and (or) the internal electrodes. The height of each post was such that the taut axon was suspended in a large bubble of solution. The temperature near the axon was monitored by a thermocouple in the solution inlet passage. Solution was removed from the chamber by suction through a vertical polyethylene tube, which controlled the height. All operations were observed through a microscope directly above the chamber. Three prisms, two adjacent to the posts and one in the chamber, provided a side view of the axon. After completion of the mechanical operations, the chamber prism was replaced by three flat platinized platinum current electrodes (two for guards and one for collecting current from the center region of membrane under potential control).

### *Solutions*

The external solutions used were (*a*) seawater (SW); (*b*) artificial seawater (ASW): 430 mM NaCl, 10 mM KCl, 10 mM $CaCl_2$, 50 mM $MgCl_2$, 5 mM Tris pH 7.4 at 25°C; and (*c*) Tris ASW (Tris substituted for Na in ASW). The standard internal perfusate was composed of 500 mM KF and 5 mM Tris, pH 7.4 at 25°C. All other solutions were composed from one of the above with additives included.

### *Internal Electrode*

A single compound electrode similar to the one of Chandler and Meves (1965) was used. It consisted of an internal potential–sensing capillary and internal current wire. The glass capillary was about 100 $\mu$ in diameter and had a 50 $\mu$ platinized platinum wire running down the entire length of its inside. The capillary was filled with 0.5 M KCl and mounted in a Lucite holder filled with 0.5 M KCl and a coil of Ag-AgCl wire. A 100 $\mu$ platinized platinum

wire was mounted "piggyback" onto the glass capillary and extended 0.75 cm beyond the tip of the capillary to provide a space clamp over the entire length of axon in the chamber solution. No correction was made for liquid junction potentials.

### *Perfusion*

A modified perfusion technique which takes advantage of the single "piggyback" electrode was suggested by Mr. Leonard Binstock. A capillary (229–279 $\mu$) was introduced into one end of the axon and moved completely through the axon and out the opposite end. Pressure was then applied to the perfusate which forced out the plug of axoplasm which accumulated during the movement through the axon. Once the flow was established, the axial wire of the piggyback electrode was inserted into the perfusion capillary which acted as a guide for the wire. The perfusion capillary was then slowly withdrawn to near its entry point while advancing the piggyback electrode into the axon. In this manner, small increments of axoplasm were cleared and replaced throughout the length of axon (1.5 cm) in the chamber. Finally, the axon was ligated just beyond the entry point of the perfusion capillary in order to prevent backflow of the perfusate out this end of the axon. Perfusion solutions containing the dye phenol red in viable axons indicated axoplasm clearance to within 10–50 $\mu$ of the membrane and flow rates from 20 to 60 $\mu$l/min.

### *Potential Control System*

The schematic of the voltage-clamp system is the same as that used on frog skin by Fishman and Macey (1969a) except that different operational amplifiers and electrodes were used. The step response (time to clamp the potential at the points in solution where the potential is being monitored) was measured during clamping of an axon to be 0.5 $\mu$sec and the time constant associated with clamping the membrane potential (time constant for charging membrane capacity) was 4.5 $\mu$sec. The series resistance between potential-sensing electrodes and membrane surfaces was determined to be 5.5 $\Omega \cdot cm^2$ and was not compensated for. A solid-state pulse generator, designed by Technical Development Section, NIMH and NINDS, and adapted to the voltage clamp by Mr. Herbert Walters, provided four independent variable-delay step commands as well as trigger pulses for synchronizing all other command signals. A triggered sawtooth generator[2] (similar to that described by Salomon [1968]) of constant amplitude provided the ramp commands as well as blanking (gate) pulses which were used in producing $I(V)$ curves on an oscilloscope. Falling ramp pulses were generated by summing a ramp and a rectangular pulse of opposite polarities but of the same duration. Falling exponential functions were obtained by applying a step of potential to a passive series capacitance-resistance circuit and using the potential response across the resistor.

### *$I(V)$ Display*

$I(V)$ curves were produced on the cathode-ray tube (CRT) of a Tektronix 524 storage oscilloscope (Tektronix, Inc., Beaverton, Oreg.) by applying $I(t)$ to the vertical and $V(t)$ to the horizontal input. In order to remove the bright spot on the CRT in the quiescent state during a clamp operation, a differential operational amplifier was placed in series with the horizontal input of the oscilloscope. This amplifier provided gain for $V(t)$ at one input and at the other input allowed the gate signal from the ramp generator to be used for deflecting the beam off

[2] Several commercial functions generators are available (e.g. Data Royal, San Diego, Calif., or Wavetek, San Diego, Calif.).

the CRT in the quiescent state. In observing the kinetics of alterations in membrane characteristics, the $I(V)$ relation was sampled at regular intervals by manual initiation of a single ramp pulse. This procedure resulted in less trauma to an axon and reduced the rate of deterioration. It also allowed use of the storage mode of the oscilloscope to observe changes as they occurred.

### *Computations*

Computation of the response of the HH axon to ramp and exponential functions was done on the GE Mark I Time Sharing System from an NIH terminal with the use of Dr. Richard FitzHugh's program (1966) for the HH formulation and his assistance in its modification for ramp pulses.

## RESULTS

### *Comparison of Squid and HH Axon Behavior for Rising Ramps*

A functional relationship between current and potential, i.e. $I(V)$, was recorded directly from an oscilloscope for linearly increasing ("rising") sweeps ($\bar{V} = dV/dt$) of potential in real axons. These data are presented in Fig. 2 together with the corresponding $I(V)$ curves computed from the HH equations for the same sweeps of potential. The current in these graphs is total membrane current, i.e., capacitive[3] plus ionic. The potential axis for the HH axon is plotted as deviation from the resting potential, whereas for the real axon the abscissa is the measured potential. There is good qualitative agreement between the two sets of curves at all ramp slopes. A significant difference occurs at high potentials for the slow ramp curves, which intersect in real axons but do not in the HH axon. This point will be discussed later. Nevertheless, it is apparent from Fig. 2 A that a ramp slope of 0.5 v/sec produces an $I(V)$ curve in which the total current is completely outward and which approximates an $I_{ss}$-$V$ curve computed from step clamp of the HH axon (Fig. 1). Similarly for fast rising ramps (Fig. 2 B) preceded by a 30 mv hyperpolarizing prepulse, the $I(V)$ curves resemble an $I_{pk}$-V plot from step clamp of the HH axon (Fig. 1). The peak inward current which develops during the fast ramp measurement (30–50 v/sec) is slightly larger than $(I_{pk})_{max}$ in step clamp (without a hyperpolarizing prepulse) of the HH axon (compare Fig. 2 B with $(I_m)_{pk}$ of Fig. 1) and is also slightly larger when compared to step clamp data from the same real axon (Fig. 6, 10°C).

The quantitative differences for slow and fast ramps probably reflect both variation from axon to axon as well as some parameter differences between *Loligo pealei* and the generalized HH axon. Furthermore, it is important to note the effect of the series resistance (between potential electrodes and membrane surfaces) on the

[3] Since membrane capacitance is a constant (Cole and Curtis, 1939), the capacitive current for a ramp in potential is a constant (independent of $V$ and proportional to $\bar{V}$) which is easily removed by displacing the oscilloscope trace $C\bar{V}$ with respect to the current axis. This has been done in some of the subsequent $I(V)$ data to obtain ionic $I(V)$ curves.

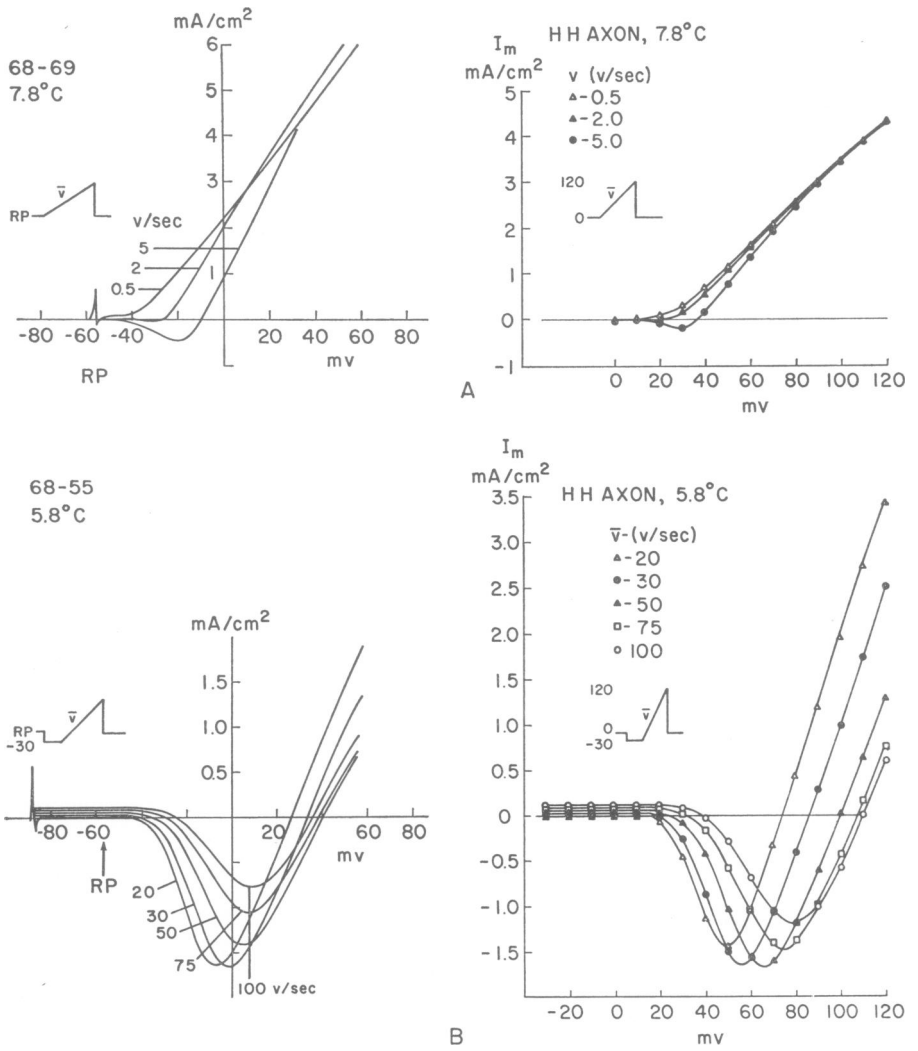


FIGURE 2 Comparison of squid axon membrane $I(V)$ data (left) with computations from the HH equations (right) for rising ramp pulses. (A) Slow ramp pulses. (B) Fast ramp pulses preceded by a $-30$ mv step. The curves from real axons in this and subsequent figures were recorded directly as multiple traces from the CRT of a storage oscilloscope and reproduced by tracing and superposing the scales. RP indicates the resting potential. The current is ionic plus capacitive. The spike in the $I(V)$ curves of real axons is an artifact produced by a former method for blanking the tracer prior to each ramp pulse.

$I(V)$ measurement. Taylor et al. (1960) showed the distortion of the step clamp-$I_{pk}$-$V$ relation as a result of not compensating for the potential drop across the series resistance. Since compensated feedback was not used in these experiments the $I(V)$ data presented are also subject to distortion.

The correspondence between predicted and measured $I(V)$ relations for rising ramp pulses gives a basis for using the HH axon to determine how well the slow (0.5 v/sec) ramp produces a steady-state potassium function, $I_K(V)$, and the fast ramp (50 v/sec) a transient sodium function, $I_{Na}(V)$. The individual ionic components of current as well as the total ionic current ($I_i$) were computed for the HH axon. Fig. 3 shows the results of these computations for each of these ramp slopes. The dashed curves represent the total ionic current (potassium, $I_K$, sodium, $I_{Na}$, and leakage, $I_L$) that would be observed for a ramp change of potential on an HH axon with each ramp slope. The constant capacitive current has been removed. $I_i(V)$ for the 0.5 v/sec ramp is essentially an $I_K(V)$ curve over the full range of potential with very small $I_{Na}$ contamination. Similarly, the fast ramp of 50 v/sec preceded by a $-30$ mv prepulse produces an $I_i(V)$ function which is identical with the $I_{Na}(V)$ curve up to the potential for peak inward current. The accuracy in representing

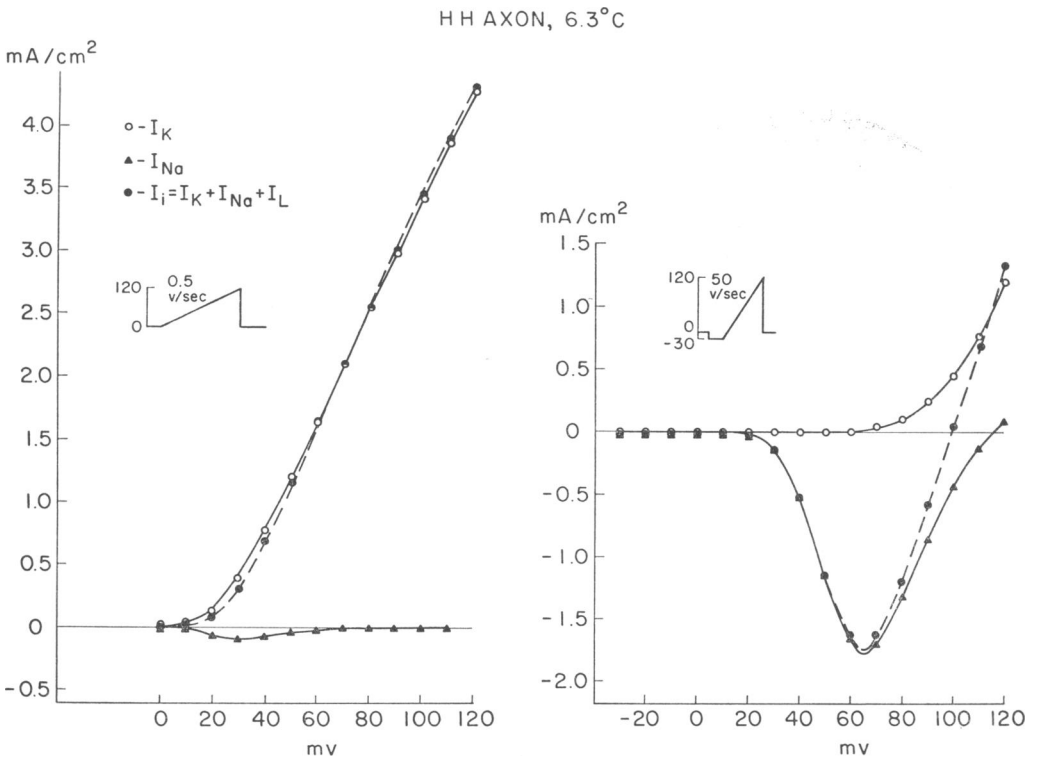


FIGURE 3 Ionic $I(V)$ curves computed from the HH equations for a slow (0.5 v/sec) and fast (50 v/sec) ramp change of membrane potential. The dashed curve in each graph represents the $I(V)$ relation (after removal of the constant capacitive current) which would be recorded directly from a CRT of an oscilloscope with these ramps as commands to a voltage-clamp system.

$I_{Na}(V)$ by $I_i(V)$ diminishes at potentials beyond the peak where the delayed outward current ($I_K$) begins to contaminate the relation. It is also of interest to note that in the fast ramp curve the computations from the HH equations show that $I_i(V)$ from $-30$ to 0 mv corresponds to $I_L(V)$; if $I_L$ so determined is removed from $I_i$, the potential at which the dashed curve ($I_i$, Fig. 3) intersects the $I_K$ curve is the sodium reversal potential ($E_{Na}$). This method of determining $E_{Na}$ can be implemented experimentally. Very fast ramps (>200 v/sec) produce $I_L(V)$ after subtracting the larger capacitive current. They can also be used to measure membrane capacitance (Palti and Adelman, 1969).

To test the hypothesis that the slow and fast ramp responses are equivalent to $I_K(V)$ and $I_{Na}(V)$ curves, the well known and highly specific inhibitors tetraethylammonium (TEA) ion (Tasaki and Hagiwara, 1957; Armstrong and Binstock, 1965) and tetrodotoxin (TTX) (Moore and Narahashi, 1967) were used to selectively reduce either the potassium conductance ($\bar{g}_K$) or the sodium conductance ($\bar{g}_{Na}$). The kinetic behavior of the $I(V)$ relation produced by the slow and fast ramps during exposure to each of the agents was recorded. In Fig. 4 A an axon in seawater (SW) was perfused internally with a solution of KF using the perfusion technique described in Methods. An ionic $I(V)$ curve was produced as a control with a single 0.5 v/sec ramp pulse. The internal perfusing solution was changed to another KF solution with 50 mM TEA added. Slow ramp pulses were applied at the times indicated subsequent to the change of solutions. Although 50 mM TEA presumably does not completely abolish the outward steady-state $I_K$ (the residual

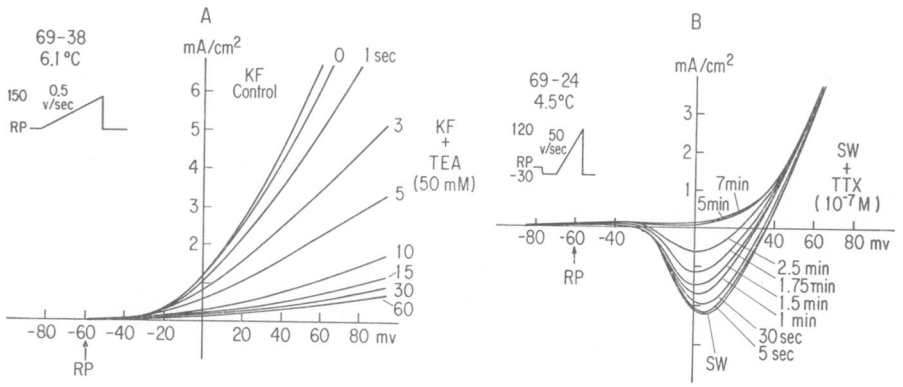


FIGURE 4 Kinetic behavior of squid axon membrane $I(V)$ characteristics recorded directly from the CRT of a storage oscilloscope in real time for a slow (0.5 v/sec) or fast (50 v/sec) rising ramp of potential after the addition of TEA to the internal (A) or TTX to the external (B) solution. (A) Upper curve is a control with the axon perfused externally with SW and internally with KF solution. Successive curves (downward) were recorded at the times indicated after the internal perfusing solution was changed to KF solution with 50 mM TEA added. (B) The lowest curve is a control of an intact axon perfused externally with SW. Successive curves (upward) were recorded at the times indicated after the external solution was changed to SW + $10^{-7}$ M TTX.

current in the 60 sec curve of Fig. 4 A seems too high to be solely $I_L$), a drastic decrease of $\bar{g}_K$ is apparent. The initial and final curves show that the slow ramp produces essentially an $I_K(V)$ relation as predicted in Fig. 3. Furthermore, these data illustrate the use of the ramp method to obtain kinetic data. The time for action of TEA depended upon the rate of perfusion and axoplasm clearance. The data in Fig. 4 A show the fastest extinction of $\bar{g}_K$ observed in these experiments. The reduction in $\bar{g}_K$ begins in less than 1 sec and is nearly complete in 15 sec. In contrast, the recovery toward the original $I_K(V)$ curve after returning to KF solution without TEA required several minutes.

Similarly, Fig. 4 B confirms the prediction that the fast ramp of Fig. 3 produces an $I_{Na}(V)$ curve. A fast ramp $I(V)$ curve was produced with an axon in SW. The SW solution was changed to SW + $10^{-7}$ M TTX and the kinetic alteration of the

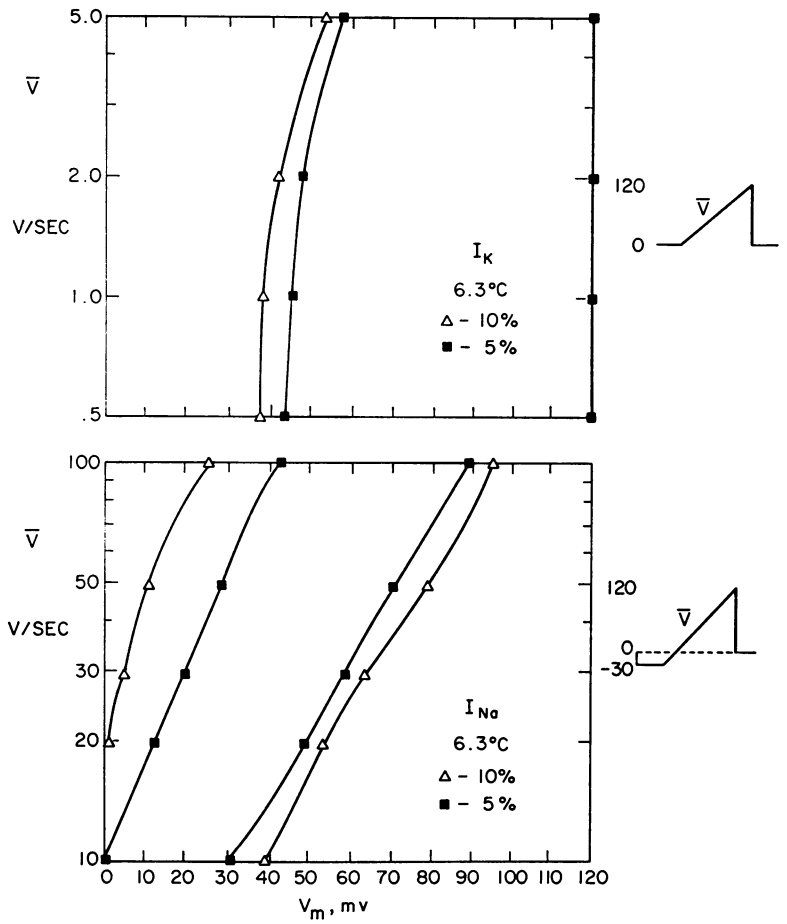


FIGURE 5 Accuracy of $I(V)$ curves produced with various ramp slopes, $\bar{v}$, in representing $I_K$ (upper) or $I_{Na}$ (lower) over the excursion in membrane potential.

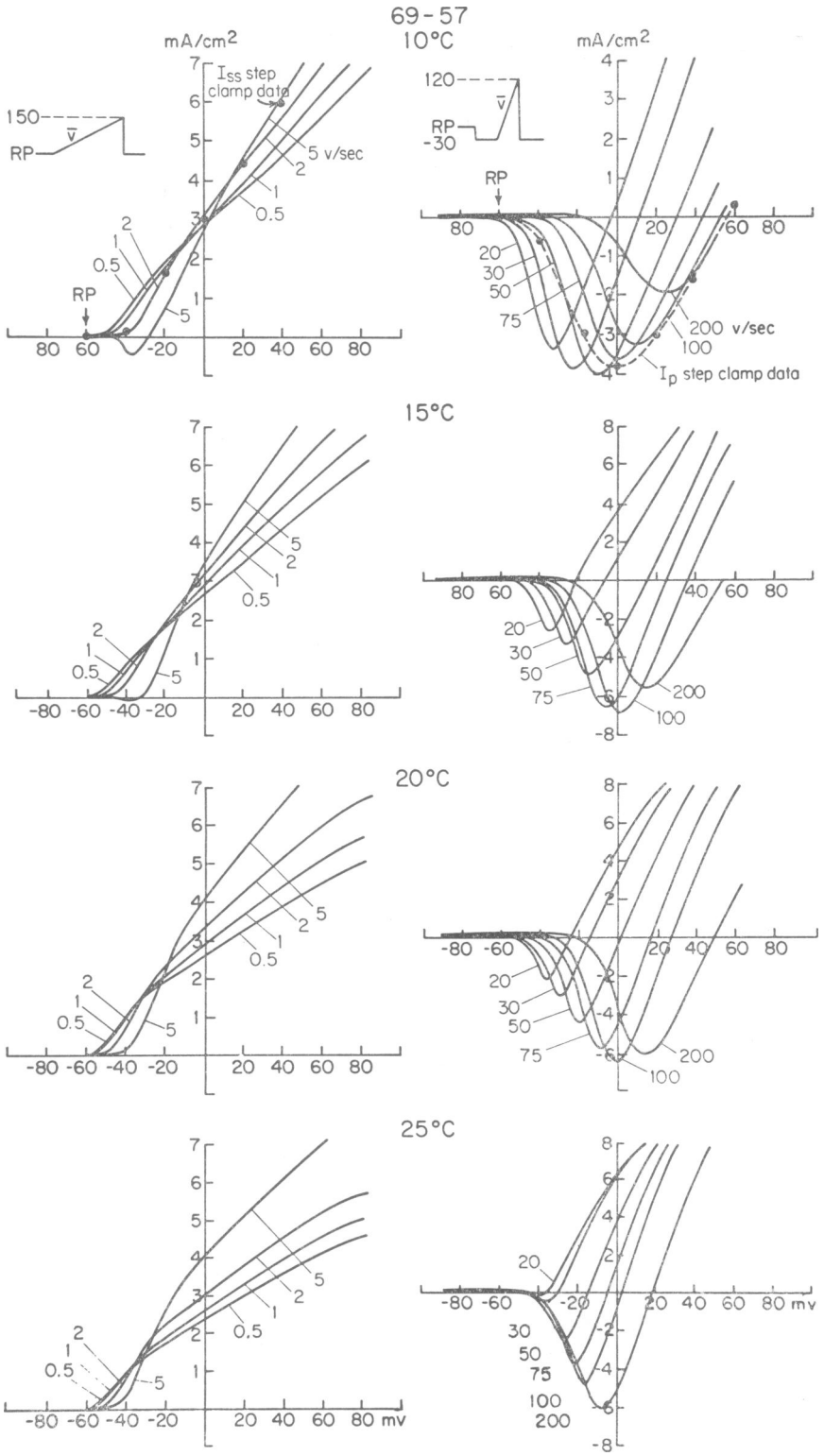
69-57
mA/cm2
10°C
Iss step
clamp data
150
RP
5 v/sec
2
1
0.5
5
120
-30
200 v/sec
100
Ip step clamp data
15°C
20°C
25°C
mv

FIGURE 6

$I(V)$ relation recorded at the times indicated. Although the kinetics of TTX are complicated by the chamber mixing time and diffusion time through the Schwann cell layers, the time for a noticeable change in the $I(V)$ characteristic with the ramp is considerably less (5 sec) than the time that would be required to collect a complete set of step clamp data. This point again illustrates well the clear advantage of the ramp method when following the kinetics of rapid alterations in the state of the membrane. The $I(V)$ relation after 7 min in TTX confirms the predicted unaltered potassium component, $I_K$ (Fig. 3), in the fast ramp production of an $I_{Na}(V)$ curve. The potential at which the $I(V)$ curve after 7 min in TTX intersects the $I(V)$ curve before TTX (although not clear in Fig. 4 B) is $E_{Na}$ since both curves contain $I_L$ plus $I_K$ .

*Ramp Slope Accuracy Limits*

Computations using the HH axon at 6.3°C to determine the range of potential over which accurate $I_K$ or $I_{Na}$ characteristics are obtained for various rising ramp slopes are summarized in Fig. 5. The total ionic current corresponds to potassium current over the widest range of potential for the lowest ramp slope (0.5 v/sec). The range of potential for accuracy in sodium current to within 10% remains fixed at about 50–60 mv for ramp slopes 20–100 v/sec. However, as the ramp slope increases the absolute voltage limits shift toward higher potentials (Fig. 5) while the magnitude of the peak of inward current reaches a maximum and then decreases (Fig. 2 B). Thus, the optimum fast ramp (50 v/sec) produces a maximum in $I_{Na}$ as well as the widest accuracy limits.

*Temperature Variation*

The previous data and computations were obtained for operating temperatures at or near 6.3°C. The data of Fig. 6 show the effect of temperature variation from 10° to 25°C on slow and fast ramp $I(V)$ curves in the same axon. In the slow ramp measurements of Fig. 2, it was noted that at high potentials the curves crossed. The same crossing is observed in the slow ramp curves of Fig. 6. The potential at which the curves intersect moves toward the resting potential with increasing temperature. It appears that this effect is similar to the observed droop in steady-state current for long, step clamp pulses. Frankenhaeuser and Hodgkin (1956) suggested that this droop is caused by an accumulation of potassium in the space between Schwann cells and the axon membrane. The same explanation seems valid for the slow ramp (long duration pulses) $I(V)$ curves which bend toward a lower conductance at high potentials.

FIGURE 6 Effect of temperature variation from 10° to 25°C on the $I(V)$ curves produced by slow and fast ramp pulses on squid axon membrane. The dashed curves in the 10°C data are from step clamp data on the same axon at 10°C for comparison to the ramp $I(V)$ data. Note current scale change for fast ramp (15°, 20°, and 25°C) data.

TABLE I
OPTIMUM RAMP SLOPES WITH TEMPERATURE

| Temperature range | Slow ramp ($I_K$) | Fast ramp ($I_{Na}$) |
|---|---|---|
| °C | v/sec | v/sec |
| 0–5 | 0.5 | 30 |
| 5–10 | 1.0 | 50 |
| 10–15 | 2.0 | 75 |
| 15–20 | 3.0 | 100 |
| 20–25 | 4.0 | 200 |

The effect of an increase in temperature would then be to increase the rate of potassium buildup so that the apparent conductance decrease occurs at lower potentials. However, despite this effect a slow ramp does give a good $I_K(V)$ relation as indicated by the action of TEA in Fig. 4 A. Thus as the potassium process speeds up with temperature, faster ramps (shorter pulse duration) may be used to produce better $I_K(V)$ curves. For example, a slope of 0.5 v/sec could be used in the temperature range from 0° to 10°C as indicated by the data of Figs. 4 A and 6 and from computations, which showed $<0.5\%$ change in accuracy for the interval 0°–10°C. However, to reduce the apparent decrease of $\bar{g}_K$, the temperature ranges over which particular ramp slopes are used could be narrowed to 5°C intervals (Table I), (Fig. 6).

The fast ramp curves are also affected by temperature. Accuracy in producing an $I_{Na}(V)$ curve, judging from Fig. 6 and computations on the HH axon, is surprisingly not diminished over temperature intervals of as much as 10°C or if the appropriate fast ramp is used in the designated temperature intervals (Table I). Thus the ramp measurement of either the potassium or sodium event is rather insensitive to large changes in the time constants as a result of temperature variation. This, of course, gives assurance that a change in conductance, which is recorded as a change in current in the $I(V)$ function, is not an apparent conductance change due to alteration in time constants. Other tests on the effect of changes of time constant (e.g. variation of external calcium concentration) o n the ramp $I(V)$ curves show that a good separation of the currents is maintained with slow and fast ramps for relatively large changes in time constants.

### *Comparison of Squid and HH Axon Behavior for Falling Ramps*

Additional ramp functions have been useful in rapidly characterizing axon membrane behavior. The most interesting one, which was suggested by Dr. Richard FitzHugh, is a "falling" ramp (a step to high potential immediately followed by a ramp which returns the potential to its value prior to the step). Fig. 7 compares the $I(V)$ relations recorded directly from real axons with the curves constructed from computations of the current response of the HH axon to the same falling ramps.

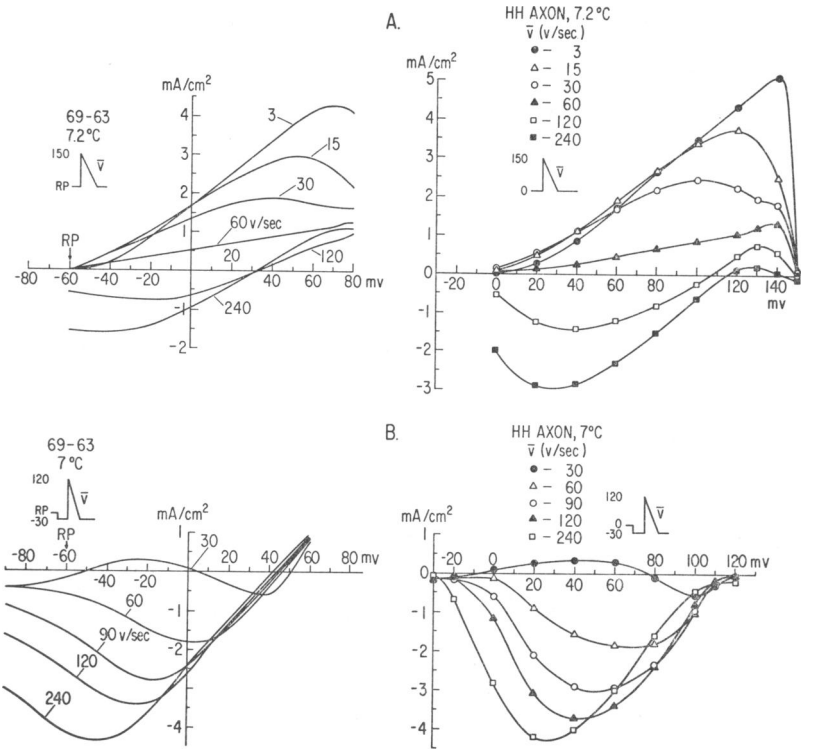


FIGURE 7 Comparison of squid axon membrane $I(V)$ data (left) with computations from the HH equations (right) for falling ramp pulses. (A) Slow falling ramp pulses. (B) Fast falling ramp pulses preceded by a −30 mv step. The capacitive current has not been removed.

The slowest falling ramp appears to produce an $I_K(V)$ curve (except for the transient shortly after the step to high potential) and the responses to fast ramps resemble $I_{Na}(V)$ curves. The HH equations were again used to compute the individual ionic components of current during the application of a slow and a fast falling ramp (Fig. 8). There are three apparent advantages in the use of these falling ramps over the comparable rising ramps. (*a*) The separation of potassium and sodium currents for the two slopes is excellent over the full range of potential (ramp excursion). (*b*) The falling ramp slope (5 v/sec) which produces an $I_K(V)$ curve is an order of magnitude faster than the corresponding rising ramp slope (0.5 v/sec). Thus the axon experiences less trauma for each ramp pulse and the apparent decrease in $\bar{g}_K$ as a result of potassium accumulation is significantly less. (*c*) The maximum inward sodium current for the 200 v/sec falling ramp is nearly twice the value obtained in step clamp with a −30 mv prepulse (Fig. 1). The explanation for this unusually large inward current is seen in Fig. 8 B where the trajectory of the product of the HH parameters $m^3$ and $h$ are plotted for step clamp and the falling ramp pulse, each preceded by a −30 mv step. The maximum value of $m^3h$ for the

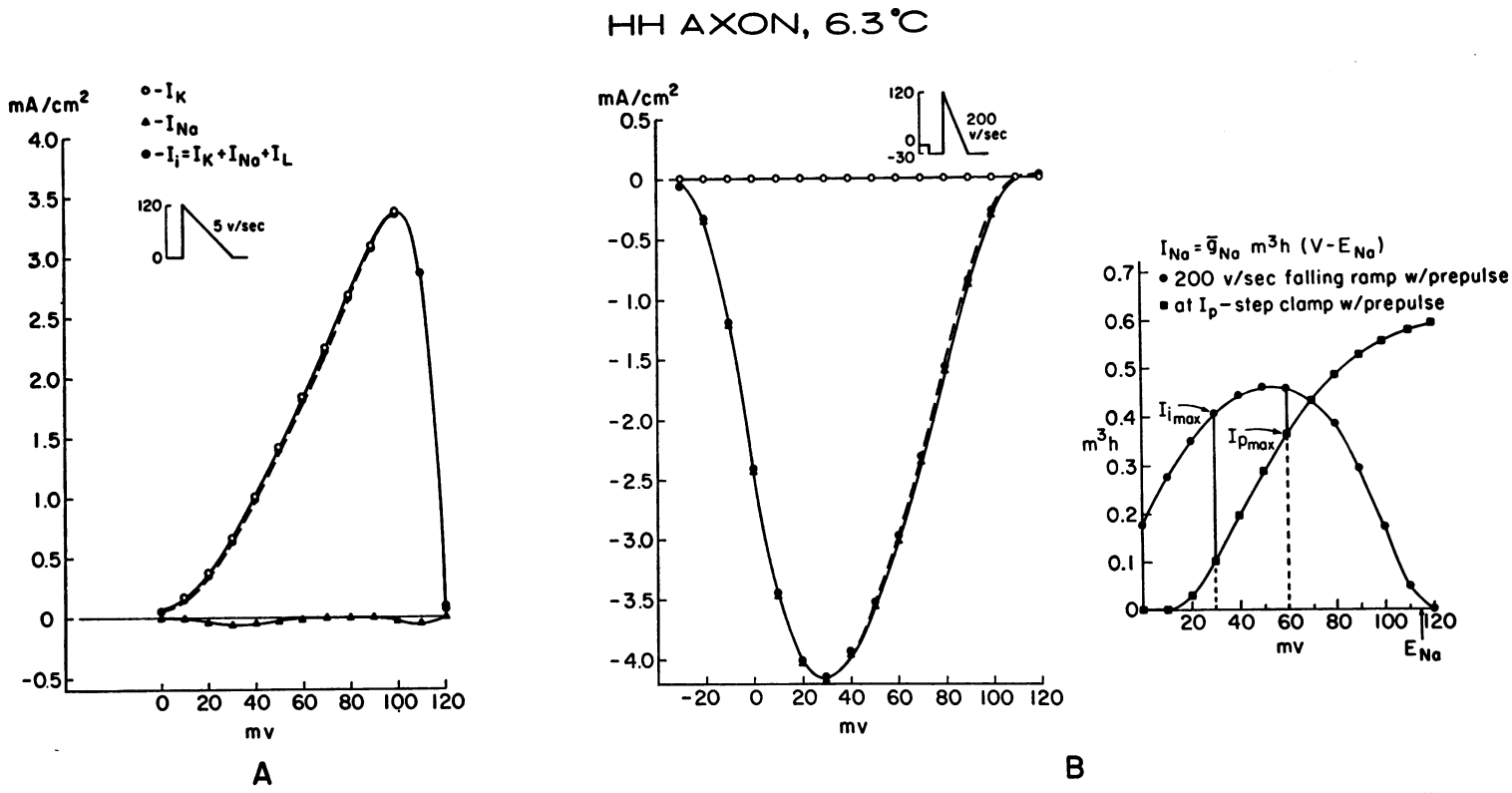


FIGURE 8 Ionic $I(V)$ curves computed from the HH equations for a slow (5 v/sec) falling ramp (A) and a fast (200 v/sec) falling ramp (B) change of membrane potential. The dashed curve in each $I(V)$ graph represents the relation (after removal of the constant capacitive current) which would be recorded directly from an oscilloscope with these ramps applied to an axon membrane. The extraordinary $I_{Na}$ for the fast falling ramp is explained by the comparison (B) of the trajectory of the product of the HH parameters $m^3$ and $h$ for step changes and a falling ramp change of potential. The falling ramp produces 2–3 times the value of $m^3h$ obtained for step clamp at potentials far removed from $E_{Na}$.

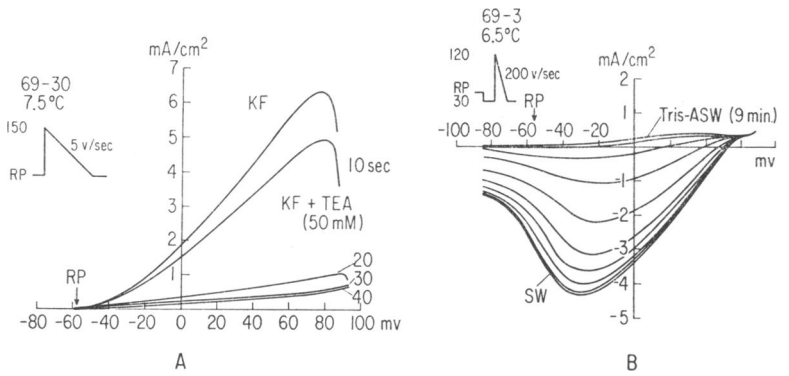


FIGURE 9 Kinetic behavior of squid axon membrane $I(V)$ characteristics recorded directly from the CRT of a storage oscilloscope in real time for a slow (5 v/sec) or fast (200 v/sec) falling ramp of potential after the addition of TEA to the internal (A) or total replacement of Na by Tris in the external (B) solution. (A) Upper curve is a control with the axon perfused externally with SW and internally with KF solution. Successive curves (downward) were recorded at the times indicated after the internal perfusing solution was changed to KF solution with 50 mM TEA added. (B) The lowest curve is a control of an intact axon perfused externally with SW. Successive curves (upward) were recorded every minute up to 9 min after the external solution was changed to Tris ASW.

falling ramp is larger and occurs at a potential further from $E_{Na}$ (115 mv) than does the corresponding maximum during step clamp. Thus $I_{Na}$, which is proportional to $m^3h(V - E_{Na})$ (where $V$ is the applied potential), is larger for the falling ramp.

Experimental test of the predicted separation of currents for the slow and fast falling ramps is shown in Fig. 9. Internal perfusion with TEA was used again to selectively reduce $\bar{g}_K$ and demonstrate the sensitivity of the 5 v/sec ramp $I(V)$ curve to $I_K$. The falling ramp can also be used (Fig. 9 A) in the same manner as the rising ramp to observe kinetic changes in $I(V)$. Fig. 9 B shows the $I(V)$ relation produced by the fast falling ramp with an intact axon in SW and every minute up to 9 min after the external SW is changed to Tris ASW (no Na). The slight outward current at high potential while in Tris ASW after 9 min is probably outward $I_{Na}$ since TTX eliminated this current. Both the extraordinary large inward $I_{Na}$ and the selectivity for sodium predicted in Fig. 8 B are thus confirmed. Furthermore, the kinetics shown in Fig. 9 B give a measure of the time required ($\tau \simeq 2$ min) to deplete the sodium pool in the space between the axonal membrane and Schwann cells.

### *Other Useful Potential Functions*

Emphasis in this paper has been placed on ramp functions because they have a number of features which enable the implementation of a direct and immediate characterization of axon membrane behavior. However, there are other functions which may have usefulness under a different set of criteria. Palti and Adelman

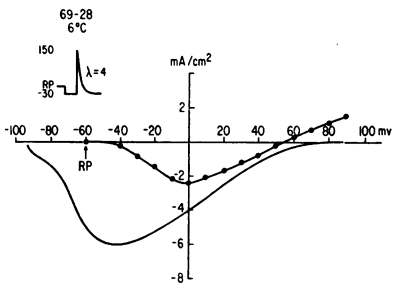


FIGURE 10 $I(V)$ relation produced by a falling exponential ($\lambda = 4$ msec$^{-1}$) on a squid axon membrane. The capacitive current has not been removed. The curve drawn through the plotted points is an $I_{pk}$-$V$ curve produced from step clamp data of the same axon.

(1969) have reported the use of periodic functions such as sinusoidal and triangular wave forms. An exponential function was suggested by Dr. Kenneth S. Cole with the motivation being that as in the falling ramp the value of $m^3h$ could be held closer to unity at potentials far removed from $E_{Na}$. The result then would be an even larger $I_{Na}$. Fig. 10 shows the $I(V)$ relation for a falling exponential preceded by a $-30$ mv prepulse. For comparison, an $I_{pk}$-$V$ curve (filled circles) from the same axon has also been plotted. The capacitive current, which is a linear function of potential for an exponential function, has not been removed for the response to the exponential. Nevertheless, the inward current is nearly 3 times larger than the $(I_{pk})_{max}$ from step clamp (Fig. 1). Further, it seems reasonable to expect that a slow-falling exponential should reduce the complications at high values of $I_K$ (Temperature Variation, p. 809).

## DISCUSSION

Although the HH formulation does give a complete description of axon behavior, few investigators go through the tedious analysis of step voltage clamp data to obtain the HH parameters. Instead, the standard way of presenting these data is in the form of two $I$-$V$ plots of points taken at the steady-state and peak inward currents of a set of step clamp current responses. From these plots, $g_K$ and $g_{Na}$ can be obtained if $E_K$ has been measured and if, after correction for the leakage current, $E_{Na}$ is determined. This, however, is an inefficient way of obtaining these data. First, there is the time required to record the current responses for a set of step changes of potential. Then, the $I_{ss}$ and $I_{pk}$ points of each curve must be identified and these data replotted as $I$ vs. $V$. The data acquisition time surely limits the rate at which changes in $g_K$ or $g_{Na}$ can be observed. If only the current response for a single step, e.g. one which elicits $[I_{pk}]_{max}$, is recorded with time, this could lead to erroneous conclusions about $\bar{g}_{Na}$. For example, $(I_{pk})_{max}$ might shift to another potential, and it would appear that $(I_{pk})_{max}$ decreased and that $\bar{g}_{Na}$ decreased when, in fact, it had not. It is, therefore, important to observe the complete $I$-$V$ relation. During rapid kinetic situations, the step function is not a suitable command function for this purpose. In addition, since step clamp data must be converted to $I$-$V$ information, the results usually cannot be assessed during an experiment. Conse-

quently, there is often wasted effort. The ramp measurement eliminates these problems. $I_K$ and $I_{Na}$ can be recorded directly and rapidly so that $g_K$ and $g_{Na}$ are obtained during an experiment. As a result, it is possible to resolve conductance changes which occur in much less than a second and to make decisions about the results during the experiment. The recording of relatively fast kinetic phenomena thus becomes feasible.

Although the interpretation of kinetic data in membranes is always complicated, it may be possible, as illustrated in Fig. 9 B, to obtain more information about the properties of compartments near the membrane and what effects they exert on membrane behavior or as demonstrated in Fig. 4 A to determine the speed of action of substances which alter or block the axon membrane processes. In general, then, ramp-forcing functions provide a convenient experimental means of observing rate processes (Glasstone et al., 1941) in membranes. In addition, the selectivity and potential variation aspects of the ramp measurement may be used to give new information about membrane events if other measurements (e.g. impedance, noise, optical, or spin label) are made simultaneously.

One of the primary features of step-voltage clamp of a squid axon membrane is the measurement of a $g_{Na}$ which is about 3 times the peak value during an action potential. As a consequence, voltage-clamp measurements can distinguish changes in $g_{Na}$ which would leave the action potential unaltered. However, the value of $(g_{Na})_{max}$ during step clamp is only 35 % of the maximum theoretical $\bar{g}_{Na}$ (Fig. 8 B). Since the fast falling ramp (Fig. 8 B) and exponential (Fig. 10) give an $I_{Na}$ of about 2 times the step clamp value, these functions provide a new level of sensitivity in measuring $g_{Na}$.

If the amount of inward sodium ions crossing the membrane during step and falling ramp clamp are compared, the step gives more (a maximum value of 25.5 pmoles/cm$^2$ per pulse at 17°C was obtained by Atwater et al. [1969] compared to the computed 15 pmoles/cm$^2$ per pulse for the falling ramp). This is because the inward sodium phase persists during the onset of potassium outflow. However, if one desired to selectively measure sodium influx (e.g. with tracers), the falling ramp should give the best results because the step would have to be terminated at $I_{pk}$ in order not to have significant $I_K$. This would reduce the total number of sodium ions crossing the membrane to 5.6 pmoles/cm$^2$ per pulse at 15°C (Atwater et al., 1969). Consequently, for tracer studies, the falling ramp may be more efficient than the step.

K. S. Cole (1968, p. 441) has, for a number of years, been in search of a method of obtaining the HH conductances and time constants either in real time or shortly thereafter during an experiment. The $I(V)$ curves generated by ramps give a real time measurement of the conductances $g_K$ and $g_{Na}$. One wonders, therefore, whether the HH time constants could also be extracted from the same or similar measurements. Dr. Cole has been successful in deriving a method which uses a triangular ramp pulse to measure the time constant, $\tau_n$, of the potassium process. The time

constant information is contained in the separation of closed loop (hysteresis) curves generated by a triangular pulse with a slope which produces a small perturbation from a steady-state characteristic. A similar method may yield $\tau_m$ and $\tau_h$; however, these attempts, which would facilitate the use of the HH formulation, are left to the future.

There is some evidence which indicates that ramp functions can be used on other preparations. Trautwein et al. (1965) applied ramps of potential to heart muscle fibers, Bennett and Grundfest (1966) to gymnotid electroplaques, and Fishman and Macey (1969 *b*, *c*) to frog skin. Mr. Leonard Binstock has confirmed most of the results presented here on the giant axon of the marine worm (*Myxicola infundibulum*).

In summary, the ramp measurement described has the following features. (*a*) The capacitive component of current is a constant, which can easily be removed. Consequently, potassium or sodium $I(V)$ curves are obtained directly without chemical separation or computer assistance. (*b*) Very fast ramps (>200 v/sec) can be used to measure membrane capacitance and leakage. (*c*) The fast ramp gives a measurement of a quasi-steady-state negative conductance which is a physical state of the membrane since time and potential are continuous and synchronous variables. (*d*) The speed of generating a complete ionic $I$-$V$ relation allows observation of the kinetics of fast or slow alterations in either potassium or sodium conductance. (*e*) It conveniently extends the measurement capability of preexisting voltage clamp systems since the only additional operation required is the integration of square pulses to obtain ramp commands.

I am very grateful to Dr. Kenneth S. Cole for many contributions to this work, to Dr. Richard FitzHugh for his computer programs and assistance, to Mr. Leonard Binstock for making suggestions and the ramp measurements on *Myxicola* axons, and to Dr. Robert E. Taylor for reviewing the manuscript.

*Received for publication 2 December 1969 and in revised form 16 March 1970.*

## REFERENCES

ARMSTRONG, C. M., and L. BINSTOCK. 1965. *J. Gen. Physiol.* **48**:859.
ATWATER, I., F. BEZANILLA, and E. ROJAS. 1969. *J. Physiol.* **209**:657.
BENNETT, M. V. L., and H. GRUNDFEST. 1966. *J. Gen. Physiol.* **50**:141.
COLE, K. S. 1968. Membranes, Ions and Impulses. University of California Press, Berkeley.
COLE, K. S., and H. J. CURTIS. 1939. *J. Gen. Physiol.* **22**:649.
COLE, K. S., and J. W. MOORE. 1960. *J. Gen. Physiol.* **44**:123.
CHANDLER, W. K., and H. MEVES. 1965. *J. Physiol.* **180**:788.
FISHMAN, H. M. 1969. *Nature (London).* **224**:1116.
FISHMAN, H. M., and K. S. COLE. 1969. *Fed. Proc.* **28**:430.
FISHMAN, H. M., and R. I. MACEY. 1969 *a*. *Biophys. J.* **9**:127.
FISHMAN, H. M., and R. I. MACEY. 1969 *b*. *Biophys. J.* **9**:140.
FISHMAN, H. M., and R. I. MACEY. 1969 *c*. *Biophys. J.* **9**:151.
FITZHUGH, R. 1966. *J. Gen. Physiol.* **49**:989.
FRANKENHAEUSER, B., and A. L. HODGKIN. 1956. *J. Physiol.* **131**:341.

GLASSTONE, S., K. J. LAIDLER, and H. EYRING. 1941. The Theory of Rate Processes. McGraw-Hill Book Company, New York.
HILLE, B. 1967. *J. Gen. Physiol.* **50**:1287.
HODGKIN, A. L., and A. F. HUXLEY. 1952. *J. Physiol.* **117**:500.
MOORE, J. W., and K. S. COLE. 1963. *In* Physical Techniques in Biological Research. W. L. Nastuk, editor. Academic Press Inc., New York. **6**:263.
MOORE, J. W., and T. NARAHASHI. 1967. *Fed. Proc.* **26**:1655.
PALTI, Y., and W. J. ADELMAN, JR. 1969. *J. Membrane Biol.* **1**:431.
ROJAS, E., and G. EHRENSTEIN. 1969. *J. Cell. Physiol.* **66**(Suppl. 2):71.
SALOMON, P. H. 1968. *E.E.E.* **16**:108.
TASAKI, I., and S. HAGIWARA. 1957. *J. Gen. Physiol.* **40**:859.
TAYLOR, R. E., J. W. MOORE, and K. S. COLE. 1960. *Biophys. J.* **1**:161.
TRAUTWEIN, W., J. DUDEL, and K. PEPER. 1965. *J. Cell. Physiol.* **66**:79.